FACTA UNIVERSITATIS
Series: **Electronics and Energetics** Vol. 34, Nº 2, June 2021, pp. 307-322
https://doi.org/10.2298/FUEE2102307Z

Original scientific paper

THE EVOLUTION OF BREAKDOWN VOLTAGE AND DELAY TIME UNDER HIGH OVERVOLTAGE FOR DIFFERENT TYPES OF SURGE ARRESTERS

Emilija Živanović, Marija Živković, Milić Pejović

Faculty of Electronic Engineering, University of Niš, Serbia

Abstract. *The results of the reliability testing of Littelfuse and EPCOS gas-filled surge arresters for different overvoltages under DC discharge will be presented in this paper. The static breakdown voltage of these gas components was estimated using voltage increase rates ranging from 1 to 10 V/s. A detailed statistical analysis of experimental data has also been done. The delay time of these components for different nominal overvoltages has been investigated as an additional aspect important for component reliability. In addition, the delay time method was used as a statistical method which can give neither ion nor neutral active states number density in the glow and afterglow. It can be employed for qualitative observation of ions and neutral active states decay in the afterglow to such low concentrations where the other methods cannot be applied. Finally, a comparison has been done between the characteristics of two gas-filled surge arresters which have the same nominal overvoltage (Littelfuse and EPCOS) from different manufacturers.*

Key words: *gas-filled surge arresters, nominal overvoltage, delay time, static breakdown voltage*

1. INTRODUCTION

Efficient overvoltage protection of electronic components and systems is very important for their proper operation. The gas-filled surge arresters (marked as GFSA in this paper) are non-linear components used in overvoltage protection. In literature it is known as surge voltage protector or gas discharge tube. Overvoltage is a phenomenon where the potential of one point of a component or device in relation to the point of zero potential is greater than allowed. Overvoltage above a certain value can endanger the safety of people who operate the devices, as well as damage the devices themselves. Besides, overvoltage above the permitted levels can lead to permanent or temporary damage to certain electronic components and devices and to the appearance of noise in

Received October 30, 2020; received in revised form March 3, 2021
Corresponding author: Emilija Živanović
Faculty of Electronic Engineering, Aleksandra Medvedeva 14, 18115 Niš, Serbia
E-mail: emilija.zivanovic@elfak.ni.ac.rs

the transmission signals. Atmospheric discharges, electrostatic discharges, commutation overvoltage, radar pulses and electromagnetic pulses of a nuclear explosion can cause overvoltage existence. These types of discharges significantly affect the telecommunication lines through which they damage components. Of all the types of overvoltage, atmospheric discharge is the most dangerous because its occurrence is unpredictable.

Overvoltage protection elements can be divided with respect to the operating voltage type into linear and nonlinear according to the manner of applying voltage on them, when the current through them increases. Linear elements for overvoltage protection are electric filters, whose most sensitive elements are capacitors. Nonlinear elements for overvoltage protection are used more than linear ones and they can be divided into three groups according to the manufacturing technology and the principle of operation. These are Transient Suppresser Diodes (TSDs), Metal Oxide Varistors (MOVs) and Gas-Filled Surge Arresters (GFSA). In order to protect against overvoltage, various combined (hybrid) schemes are sometimes used [1].

Today, the most widely used GFSA consists of two or three electrodes that are enclosed in a ceramic or glass housing [1]. The distance between the electrodes is the order of a millimeter or part of a millimeter. As the insulating material, either noble gases (argon, neon, krypton or xenon) or their mixtures at pressures from 100 Pa to 70 kPa are used. The major drawbacks in GFSAs application are their delay time and cut off delay upon voltage disconnection as well as relatively large deviation in breakdown voltage, which goes up to 20% with respect to values usually found in datasheets [2,3].

Time delay method proved to be a valuable tool for Littelfuse GFSA reliability testing [4]. The continuation of our research relates to a detail analysis of these gas components and further extends to similar components manufactured by EPCOS at the same operating voltage of 230 V. On this occasion, a similar analysis was performed with the possibility to comparing the new results with previously used components as well as with characteristics from the datasheet [2,3]. The static breakdown voltage was estimated for all used samples by discretized dynamic method. In addition, the results of testing the reliability of these components, which implies determining the components' static breakdown voltage and delay time for the different overvoltage, as well as the different relaxation time, will be also shown. Further, the influence of overvoltage on the reliability of GFSA will represent, as well as a detailed statistical analysis of the obtained experimental results.

2. RELATED WORK

Previous research on GFSA has reflected that the most commonly examined types of it were SIEMENS and CITEL. Also tests performed in the field of ionizing radiation are widely represented in the literature [5,6]. The possibility of stabilizing the static working point of the GFSA by adequately selecting the parameters that are important during their fabricated was sought. This analysis has a practical importance to their manufacturer and provides a much better understanding of the pre-breakdown effects in gas at low pressure. The operating voltage of GFSA used in the experiment was 230 V [7]. The paper [8] examined the influence of the type of noble gas, gas pressure, inter-electrode gap, electrode material and the type of electrode surface processing, as well as the change of absorbed dose rate in radiation field on the operation of GFSA. Such an extensive analysis of

the impact of various parameters is performed due to their wide application in telecommunications systems, space technology and military industry.

In addition, this type of testing of GFSA is related to the period immediately before the breakdown, but there are published papers that show the results related to the contribution of positive ions and neutral active particles remaining during the previous breakdown and discharge in the gas, using the delay time method [9,10]. This statistical method can provide the qualitative separation of contribution of different particle species which can induce the secondary electron emission processes, which lead to initiation of breakdown in insulation gas. CITEL, SIEMENS and EPCOS are types of used gas-filled arresters in previous research at operating DC voltage in range of 220 to 250 V.

3. Experimental Details

3.1. Gas-filled surge arresters

The gas-filled surge arrester samples used in this work for the experiment were chosen from two manufacturers – Littelfuse and EPCOS. Littelfuse GFSA are designed with typical value of DC breakdown by:

- 285 V DC (in this paper marked as LF1)
- 230 V DC voltage (designated as LF2).
- 250 V DC voltage (in this paper marked as LF3).
- 350 V DC voltage (designated as LF4).

Aside from Littelfuse GFSA, there have also been done experiments with EPCOS GFSA which is designed to operate at the voltage of:

- 230 V DC voltage (designated as EP).

The technical characteristics of the GFSA mentioned above are listed in detail in Table 1 [2,3].

Table 1 Device specifications (at 25°C)

Device	Breakdown voltage in the DC mode (V)	DC Breakdown – typical (V)	Insulation Resistance (GΩ)	Capacitance (pF)
LF1	230 – 340	285	10	1.5
LF2	184 – 276	230	1	1.5
LF3	200 – 300	250	10	1.5
LF4	280 – 420	350	10	1.5
EP	184 – 276	230	10	1.5

The components' geometry is shown in Fig. 1. Inter-electrode space d is close to 6 mm. Precise information about gas type and pressure could not be obtained. However, manufacturer states that GFSA is filled with neon and/or argon to the pressure below atmospheric. With respect to this, further analysis of physical processes will be focused on noble gases in general at low pressures.

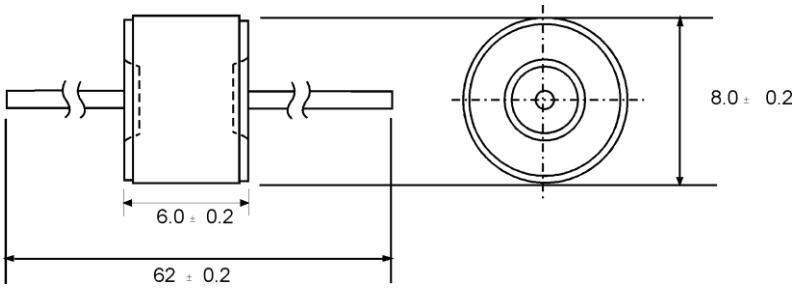

Fig. 1 The geometry of gas-filled surge arrester

3.2. Measurement system for breakdown voltage estimation

Widely established definition of the breakdown voltage U_b considers that it is the voltage applied on gas component, which induces the gas transition from non-self-sustaining to self-sustaining discharge. Due to statistical nature, breakdown voltage is not a strictly predefined value. Many different factors may influence its value [11,12]. Those are for example, the presence of external ionization source (such as X, gamma or UV source), electrodes precondition [13], ambient temperature, electrode's shape and product of inter-electrode distance and gas pressure [14,15], and many more. Considering this, gas components, GFSA in our case, manufacturers usually give the expected breakdown voltage in the datasheets, with tolerance, which goes up to 20%. From the statistical point of view, it is of great importance to determine the breakdown voltage on the onset of breakdown, i.e., the voltage for which breakdown probability is still kept at zero value. This value is referred in the literature as the static breakdown voltage U_s and there are several methods for its determination. In our experiments, we used discretized dynamic method. Estimation of static breakdown voltage is important due to the scaling of the overvoltage in relation to it.

Unlike dynamic method [16], which considers the application of linear ramp signal on gas component until breakdown, discretized dynamic method requires the application of stepped voltage on the diode until breakdown, while voltage step U_p and its duration t_p are predefined (see Fig. 2 below). In our experiments voltage step was fixed to 0.1 V. The duration of the steps was varied from 0.01 s up to 0.1 s. Correspondingly, the voltage increase rates $k = U_p/t_p$ ranged from 1 to 10 V/s. This choice of voltage increase rate increases the resolution in measurement accuracy.

The block diagram of electrical system for breakdown voltage measurement along with signals on gas diode for three successive measurements is presented in Fig. 2.

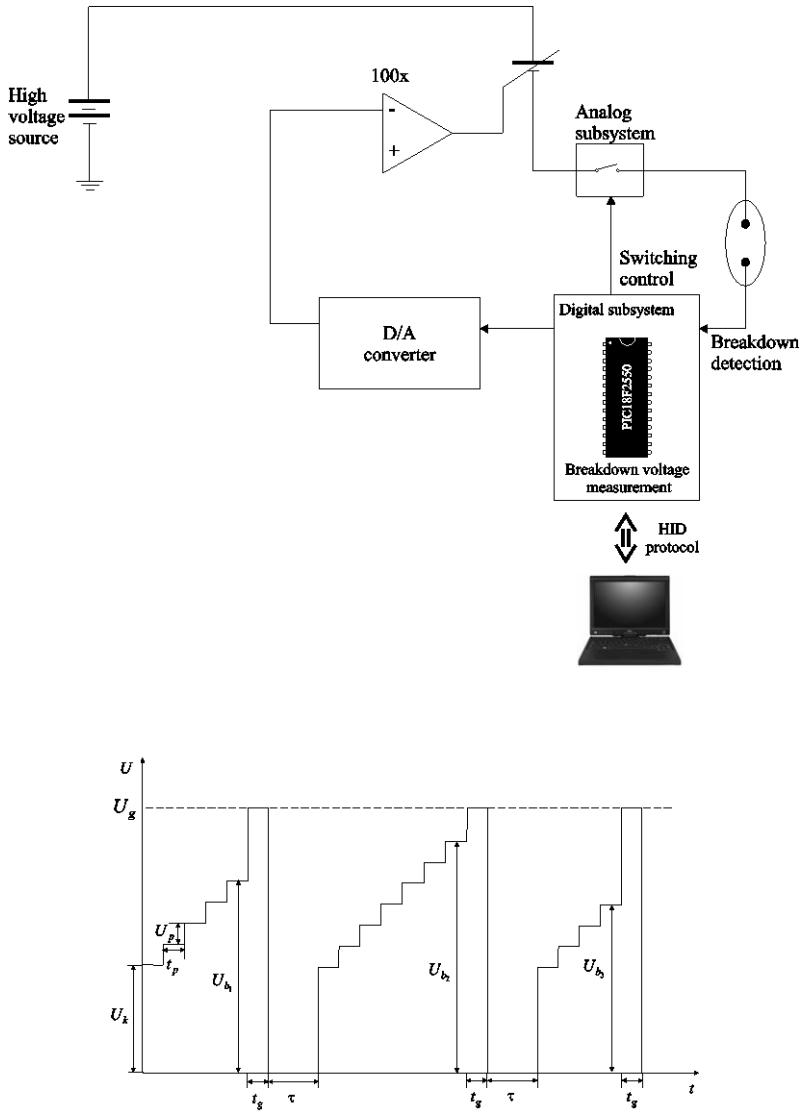

Fig. 2 Block diagram of a system for breakdown voltage acquisition: U_k - significantly smaller than the expected breakdown; U_g - value to which the voltage rises

As it can be seen from Fig. 2, the voltage on gas device is raised in steps until breakdown. Computer based control and acquisition system has been set up to increase voltage in steps of certain duration until the breakdown voltage is established and recorded, and to do so sufficient number of times so that a good statistic for the measured quantity has been achieved.

3.3. Measurement system for delay time measurement

Memory curve is the dependence between delay time and relaxation period. Due to statistical nature of delay time, it is necessary to perform large series of measurements and use the mean values of delay time as reference values. In our experiments, we used a series of a hundred delay time measurements for different relaxation periods. The relaxation periods were chosen according to logarithmic scale until the memory curve saturation. The block diagram of measurement system along with signals on GFSA for three successive measurements is presented in Fig. 3. System structure can be divided into two separate subsystems, analog and digital. The main purpose of analog subsystem is to provide fast and accurate voltage switching on GFSA. Digital subsystem, on the other hand, is responsible for measurement data collection and storage as well as the measurement control and execution.

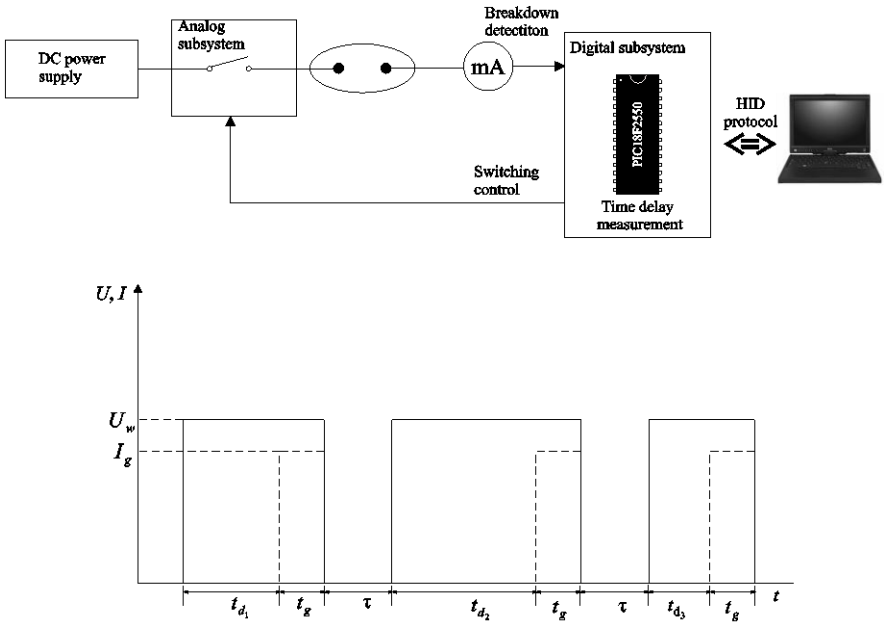

Fig. 3 Block diagram of a system for delay time acquisition

Measurement is executed in a following manner. The series of constant voltage pulses were applied on the component, while elapsed time between the voltage pulse application and breakdown was measured. Measured delay times were stored in memory and voltage pulse was maintained on diode for the time t_g in order to maintain the same conditions for every measurement. After that, the gas component was disconnected from the relaxation period τ. The procedure was repeated for a desired number of times, for different relaxation periods.

4. RESULTS AND DISCUSSION

4.1. Analysis of static breakdown voltage

Special attention in this paper will be focused to two basic characteristics of GFSA. Static DC breakdown voltage is one of them. It should be noted that the static breakdown voltage is the starting point for further overvoltage determination. And its meaning should not be confused with DC breakdown voltage from the datasheet.

Its estimation for each of used components was performed applying a dynamic discretized method [16]. It is based on a linear fit of the experimentally obtained dependence $\overline{U}_b = f(k)$, where $\overline{U}_b$ is the mean values of a thousand measured data of breakdown voltage and k is the voltage rate. The results represented in Figs. 4 and 5 show the mean value of breakdown voltage as a function of voltage increase rate for Littelfuse (for four different components) and EPCOS GFSA, respectively. The estimated static breakdown voltage is shown in all figures.

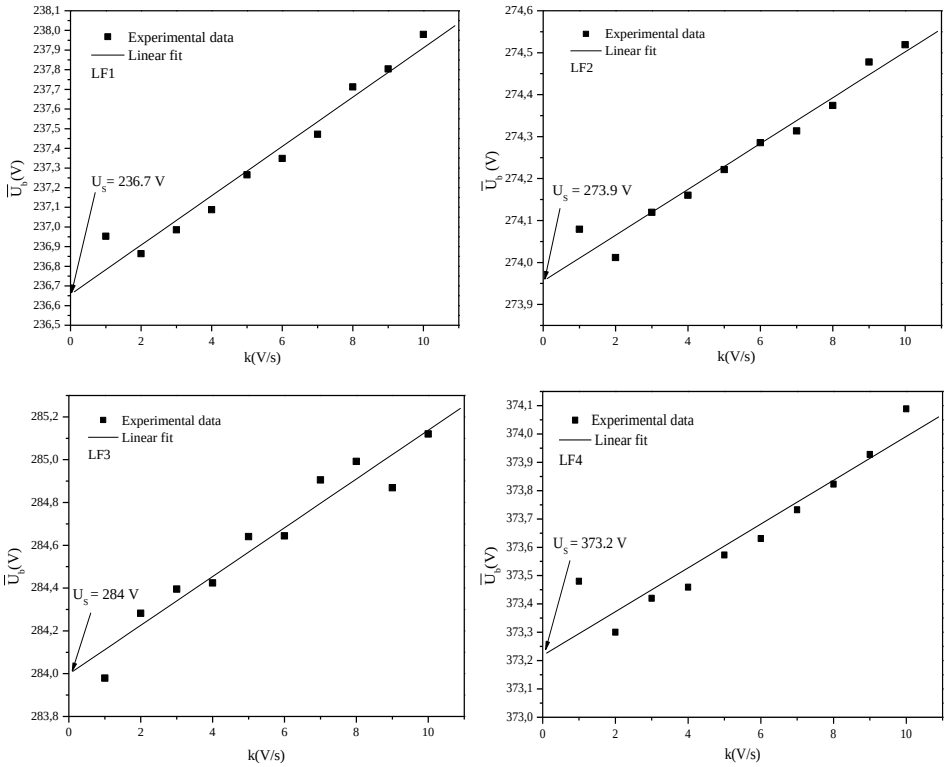

Fig. 4 Mean value of breakdown voltage as a function of voltage increase rate for Littelfuse GFSA

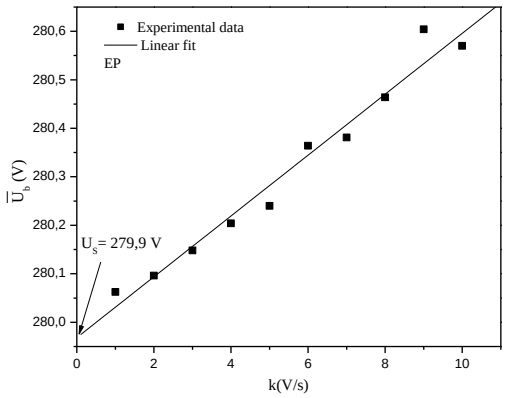

Fig. 5 Mean value of breakdown voltage as a function of voltage increase rate for EPCOS GFSA

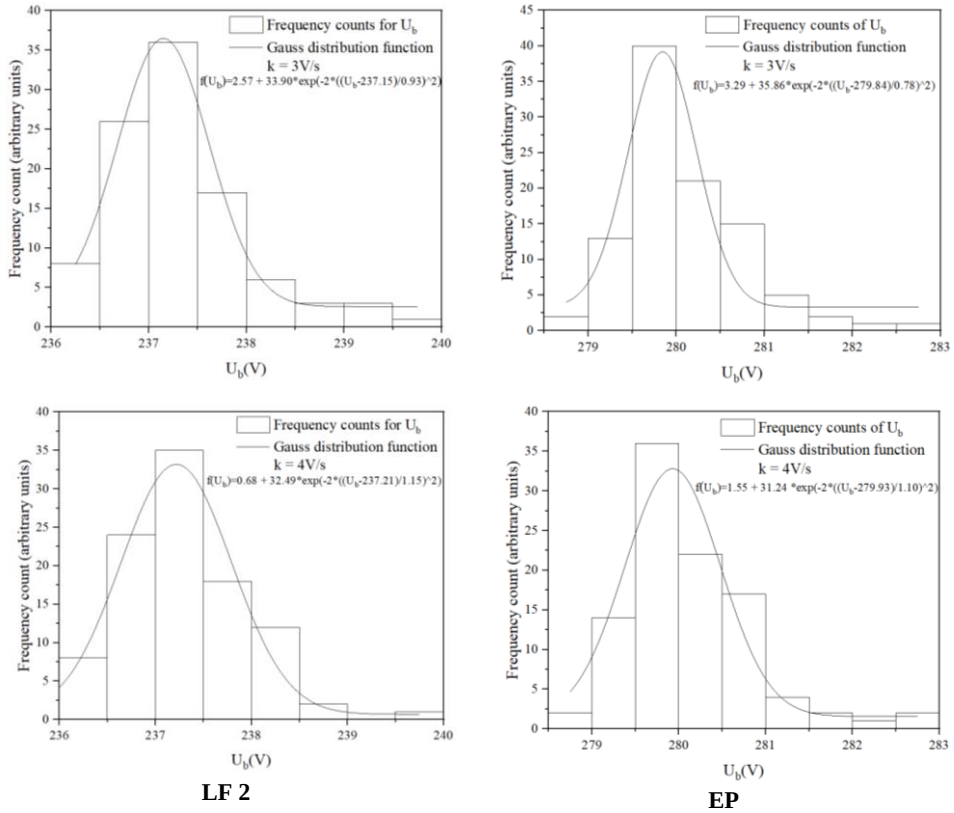

LF 2 **EP**

Fig. 6 Histograms and fitted distribution density of dynamic breakdown voltage for LF2 and EP GFSA for k = 3 and 4 V/s

In literature, in the analysis of the breakdown voltage in gas tube filled with noble gases and nitrogen, it was shown that the breakdown voltage is a statistical quantity with Gaussian distribution function. This method also takes into account the stochastic nature of the breakdown voltage. Namely, even at low voltage rise rates in a series of repeated measurements under the same experimental conditions, the obtained data will have different values. This confirms the fact that the breakdown voltage has a statistical nature with a certain distribution due to stochastic processes in the gas. This statement can be observed in Fig. 6, which shows a histogram of relative frequencies of experimental data of breakdown voltage (a thousand measurements for each voltage increase rate) as well as Gaussian distribution function. The breakdown voltage represented in this figure was obtained for voltage step $U_p = 0.3$ and 0.4 V and its duration $t_p = 0.1$ s. As mentioned above $k = U_p/t_p$ and increase rate was $k = 3$ and 4 V/s, respectively (the details about the increase rate estimation can be found in paper [16]). A similar tendency was obtained for the other k.

It should be expected for very small k that U_s has a constant value. But, the application of statistical χ^2 test, as well as R^2 correlation coefficient, (shown in the Table 2) present a good agreement between Gaussian distribution function and experimental data. A complete analysis was performed for all samples used in the experiments, but a detailed statistical analysis was shown for GFSAs marked as LF2 and EP that are at the same operating voltage of 230 V DC.

Table 2 χ^2 and R^2 values for analyzed GFSA

Device	k (V/s)	χ^2	R^2
EP	3	24.21	0.91
EP	4	19.58	0.92
LF2	3	1.18	0.99
LF2	4	9.31	0.96

4.2. Analysis of delay time

The delay time existence could be the main problem in usage of GFSAs. Due to stochastic nature of breakdown process breakdown doesn't appear instantly upon voltage application on GFSA. The time elapsed between the moment of application of voltage higher than breakdown voltage, and the moment when the GFSA current starts to flow is called the delay time t_d.

The delay time consists of the statistical time delay t_s and the formative time t_f, i.e., $t_d = t_s + t_f$ [17,18]. Statistical delay time is the time interval between the moment of operating voltage application and the appearance of a free electron which initiates the breakdown. Formative time is the time taken from the end of the statistical delay time to the onset of breakdown, characterized by the collapse of the applied voltage as a transition self-maintained glow [17]. The various parameters have an influence on delay time, but the most important factor is the relaxation time τ which represents the time interval between two successive measurements when there is no voltage on the used component [18]. This dependence, $\bar{t}_d = f(\tau)$, is usually called the memory curve. It can be divided into three distinctive areas, those are plateau, the growth of delay time with relaxation and saturation. Different mechanisms of breakdown initiation play dominant role in each range of the memory curve. However, the existence of a memory curve is undesirable when studying the reliability of gas-filled surge arresters, which will be discussed later in the paper.

Since the GFSAs' manufacturers do not provide exact specification of the gas composition in the technical documentation, it can only be found that these are noble gases, and that argon and neon are most often used for this purpose. During the experiment itself, a reddish-orange glitter is noticed, which is a hint that these are noble gases. The experimentally obtained memory curves for Littelfuse GFSA (Fig. 7) can be compared with those previously obtained for argon and neon [19,20]. It can be seen that the shape of the curve is similar, i.e., that the plateau appears as well as the area of increase delay time with the period of relaxation. The plateau area itself is characterized by the constancy of the delay time with relaxation regardless of the overvoltage. Only a decrease in the delay time with an increase in overvoltage is observed. As far as the plateau area is concerned, in this range of relaxation there is a high concentration of positive ions in the gas, which are formed both during discharge and afterglow. The processes that are possible with noble gases in which positive ions are formed, are responsible for maintaining discharge are listed in Table 3 [21].

Table 3 Positive ions' creation

Process	*Reaction*
direct ionization	$e + X \rightarrow X^+ + 2e$
stepwise ionization of metastable atoms by electron impact	$e + X^m \rightarrow X^+ + 2e$
metastable-metastable collision ionization	$X^m + X^m \rightarrow X^+ + X + e$
	$X^m + X^m \rightarrow X_2^+ + e$
excited atom-ground state atom collision	$X^* + X \rightarrow X_2^+ + e$
three-body collision (ion conversion)	$X^+ + 2X \rightarrow X_2^+ + X$
ion recombination between electron and molecular ion	$e + X_2^+ \rightarrow X^* + X \rightarrow X^m + X$
diffusion on the device wall	$e, X^m, X^+, X_2^+ \rightarrow wall$

In reactions represented above (Table 3), X is the ground state's atom of noble gas, while X^* and X^m signify resonant excited and metastable level, respectively. As X^+ and X_2^+ are marked positive ion in atomic and molecular form, respectively.

In Figs. 7 and 8 families of delay time vs. relaxation (memory curve) dependencies are shown, for all Littelfuse samples as well as for EPCOS GFSA, respectively. Dependencies were recorded for different overvoltages. The overvoltage is most often expressed in percentages and defined as $(\Delta U / U_s) \cdot 100$ %, where ΔU is the difference in operating voltage U_w ($U_w > U_s$) and static breakdown voltage, i.e., $\Delta U = U_w - U_s$. The aim of this study was to examine the effect of the applied voltage to the delay time in the function of relaxation time because of determined overvoltage range corresponding to safe component operation.

The memory curves' plateau (see Figs. 7 and 8) is a consequence of positive ions' recombination formed by first five reactions from Table 3. Atoms and molecules in ground and metastable state have also been included in the secondary electron emission (SEE) process, but because of their electroneutrality had much smaller contribution. The rapid growth of delay time can be observed in some cases. It is a consequence of a change in mechanisms yielding the dominant influence in the SEE process. Significant decrease of ion

concentration as well as longer recombination time of neutral particle is the main cause of sudden t_d rise.

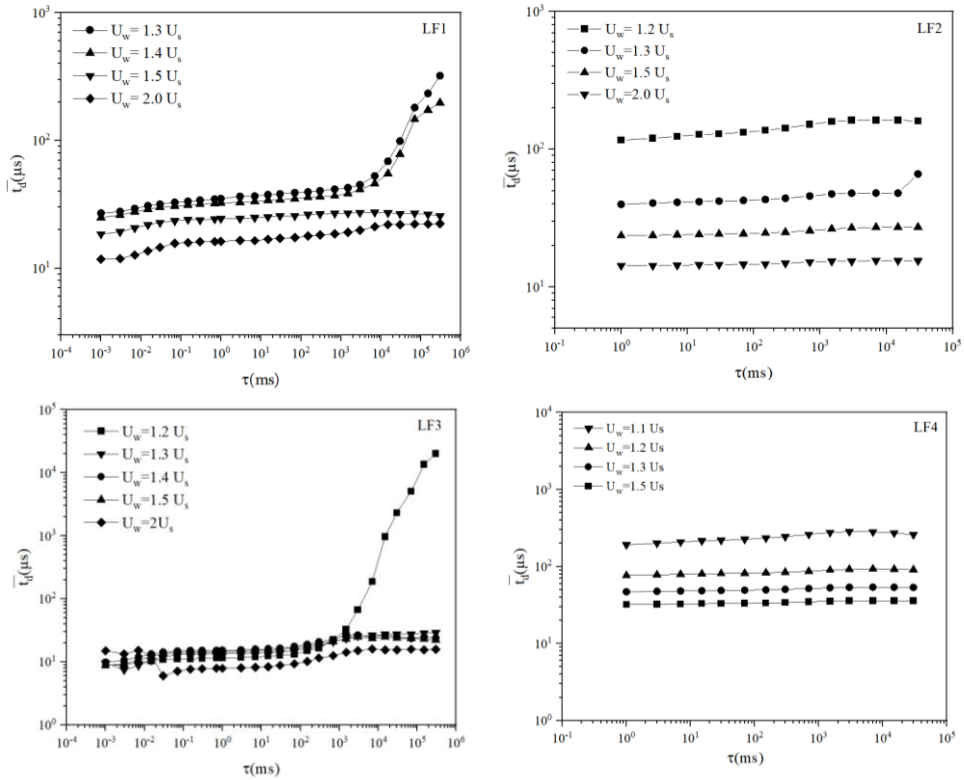

Fig. 7 Mean value of delay time as a function of relaxation time for different overvoltage for Littelfuse GFSAs

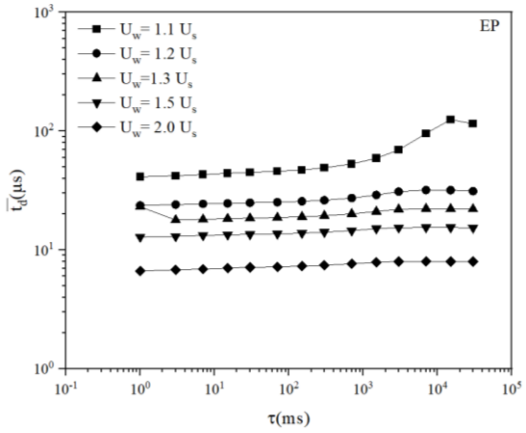

Fig. 8 Mean value of delay time as a function of relaxation time for different overvoltage for EPCOS GFSA

Two conclusions can be drawn from the presented results. The first one is a tendency toward delay time decrease with increasing overvoltage for all GFSAs. It has been previously tested and confirmed for gas-filled tube that by increasing the voltage, the probability of a breakdown in the gas increases as well as the probability that the secondary electrons released from the cathode lead to a breakdown [22-24]. When the yield of electrons in a gap is a constant, the mean value of delay time is inversely proportional to the breakdown probability [22]. It has also been shown that the breakdown probability increases with increasing overvoltage, which is manifested by a decrease in the mean value of delay time.

In most of the experimental results, the obtained characteristics do not show an increase in delay time, that is expected. Since delay time is practically independent of the relaxation time τ it can be concluded that tested components worked reliably in the whole range of tested relaxation periods. However, it can be seen in Fig. 7, that samples LF1 and LF3 show different tendency for lower values of overvoltage. Namely, sample LF1 shows significant increase in delay time for relaxation period longer than 7 s for overvoltages $1.3U_s$ and $1.4U_s$, while sample LF3 shows similar behavior for relaxation longer than 700 ms and overvoltage $1.2U_s$. With respect to above mentioned, it can be concluded that these components are not reliable for operation in the area of significant increase of delay time. EP sample in Fig. 8 shows similar behavior for relaxation about 1.5 s and $1.1U_s$ overvoltage although increase in delay time is smaller than for LF1 and LF3 samples.

In order to establish overvoltages below which components are not reliable, the delay time method allows evaluating the delay time of these components. Namely, the memory curves (Figs. 7 and 8) indicate to values of GFSA, i.e., approximate from 10 μs to 30 μs for LF1, as well as in the range of 15 μs to 200 μs for LF2, around 10 μs for LF3, from 30 μs to 300 μs for LF4, and between 80 μs and 400 μs for EP.

As the GFSAs of both manufacturers showed a deviation in the results for relaxation times of about 10^5 ms, this required further statistical analysis. Figs. 7 and 8 also indicate that for some overvoltage there is an increase in delay time with increasing relaxation time. This is something which indicates instability in the operation of the component with respect to the delay time. In the earlier results [22-25] of the memory effect study, it can be seen that in the region of increase for most experimental conditions t_s is less than t_f, as well as that the standard deviation of t_f is very small, in the analysis of total delay time, in the first approximation we can assume that under constant experimental conditions, it is deterministic. In this case, the delay time becomes the sum of one deterministic t_f and one stochastic quantity t_s, so it takes on its stochastic character from the statistical delay time. It has been shown earlier [18] that the statistical delay time has an exponential distribution, which is based on the physical nature of the processes that occur in the gas. In the physical literature, the exponential distribution is based on the so-called Laue distribution. It is represented by diagrams - lauegrams, where N is the total number of delay time measurements, and $n(t)$ represents the number of measured delay time whose values are greater than t. This corresponds to the drawing of the function

$$\ln R(t) = -\lambda(t - t_f),$$

where $R(t) = 1 - F(t) = 1 - \int_{t_f}^{t} \lambda \exp[-\lambda(x - t_f)]dx$, is the function that represents the probability that a breakdown in the gas will occur after time t. Since $\lambda = 1/\overline{t_s}$, Laue distribution is usually written in the form [26]

$$\ln \frac{n(t)}{N} = -\frac{t - t_f}{\bar{t}_s}.$$

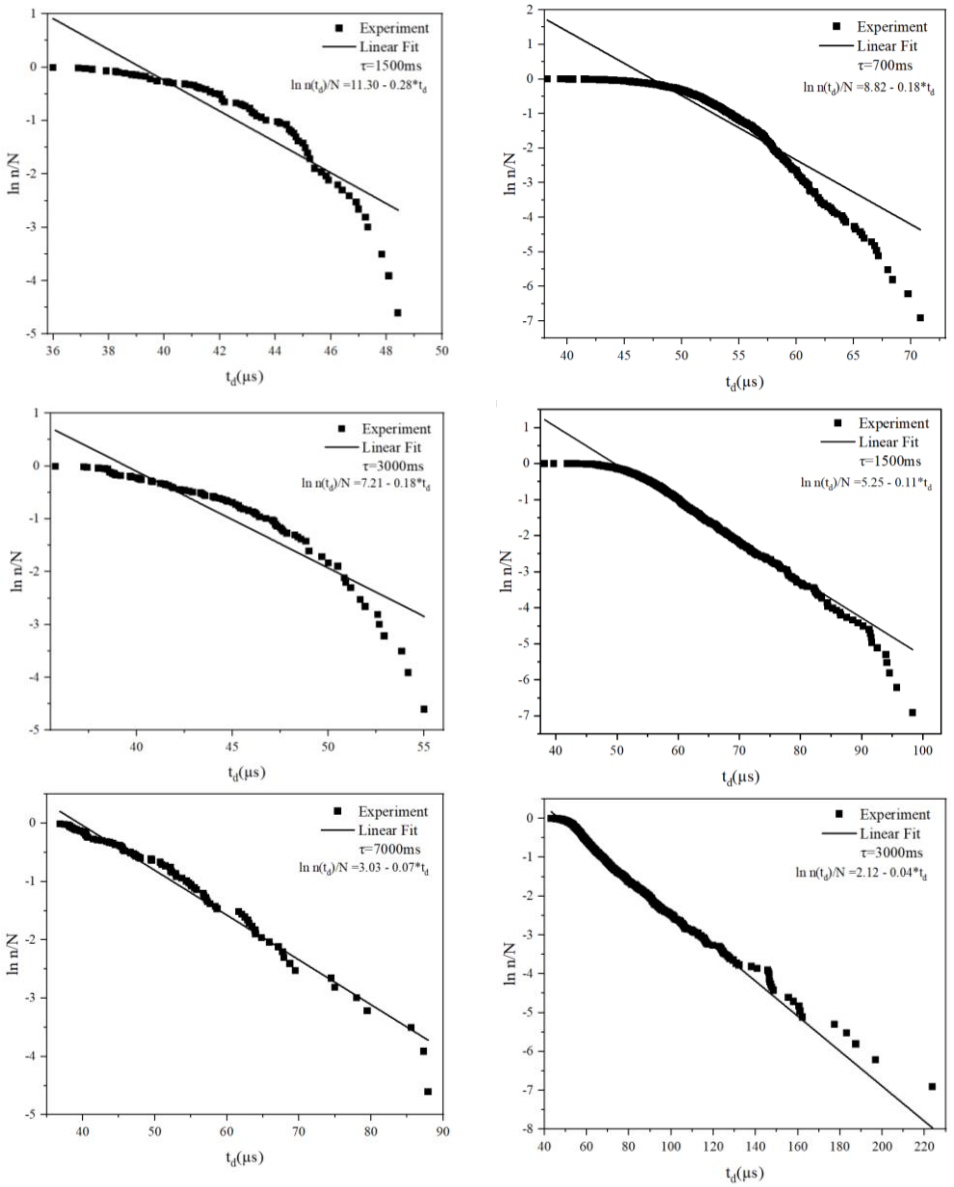

LF2 **EP**

Fig. 9 Lauegrams of the relaxation time for the previously observed deviation of GFSA of both manufacturers where the delay time increases suddenly and where the operation of the components is not reliable

This expression shows that the mean value of the statistical delay time, and thus the electron yield, can be obtained from the slope of straight line, and the formation time is cut off on the t_d - axis. On lauegrams, the linear fit is obtained using the least squares method when determining the distribution parameters. The correlation coefficient was determined for each data set. It connects the data of two features, in this case ln $n(t_d)/N$ and t_d, and represents a quantitative measure of the agreement of the experimental data for the delay time with the exponential distribution. Fig. 9 represents the lauegrams for those relaxation times for which the deviation in Figs. 7 and 8 is observed. For these relaxation times, the delay time increases suddenly and for these values the operation of the components is not reliable. A detailed statistical analysis was performed to check whether it was a measurement fault or physical processes occurring in the gas. If there is a good Laue distribution, i.e., if R^2 correlation coefficient is close to unity, it means that scattering of experimental delay time data exist. Then the memory curve is expressed, so from a technical point of view, the arrester is not good. For smaller R^2, the data is more difficult to describe by the Laue distribution, so there is no memory curve and the delay times are small, so the arrester is reliable.

The results of the used statistical Pearson's test confirm this, as well as the fact that with the growth of relaxation time. Confirmations of these facts can be seen in Tables 4 and 5. The first one refers to the analysis of experimental data of the gas-filled surge arrester marked as LF2, and the second to the EP.

Table 4 Pearson's test and R^2 for LF2

τ	Pearson's r	R^2
700	-0.92	0.85
1500	-0.98	0.97
3000	-0.99	0.99

Table 5 Pearson's test and R^2 for EP

τ	Pearson's r	R^2
1500	-0.90	0.81
3000	-0.92	0.85
7000	-0.99	0.97

5. CONCLUSION

Based on all of the above, the following can be concluded. The paper investigates the reliability testing of Littelfuse and EPCOS gas-filled surge arresters. Using the dynamic discretized method for different voltage increase rates from 1 to 10 V/s, the static breakdown voltage was precisely estimated. Components' delay time has been determined for different nominal overvoltages using delay time method.

The mean value of breakdown voltage as a function of voltage increase rate for all GFSAs has been shown. In addition, histograms and fitted distribution density of dynamic breakdown voltages for LF2 and EP GFSAs, that are at the same operating voltage of 230 V DC, for $k = 3$ and 4 V/s are shown. It is evident that the breakdown voltage for these GFSAs is a statistical quantity with Gaussian distribution function, as presented.

The delay time of the GFSAs is determined from the obtained experimentally memory curve. Figs. 7 and 8 show those dependencies, the mean value of delay time as a function of relaxation time for different overvoltage for Littelfuse and EPCOS GFSAs.

As it can be observed, in the case of LF1, for overvoltages greater than 40% this type of surge arrester works reliably. Also, for overvoltages less than 40% it also works reliably for relaxation times up to 7 s. For LF2, we can notice that the device works reliably for overvoltages greater than 20%. In the case of LF3, reliability is shown for overvoltages over 30%. For overvoltages less than 30% it works reliably up to 1.5 s of relaxation time. Also, LF4 shows very good reliability for overvoltages over 10%. Finally, EPCOS device has the reliability for overvoltages over 20%, while under 20% unreliability is shown for relaxation times over 1.5 s.

Additionally, the previous results which show an increase in delay time with increasing relaxation time were used for further statistical analysis. The Laue distribution of these data is represented by lauegrams in Fig. 9. It shows that the mean value of the statistical delay time, and thus the electron yield, could be obtained from the slope of a straight line, and the formation time is cut off on the t_d - axis.

Further analysis is planned in order to continue research with the goal of comparing already obtained results with additional analysis of ionizing radiations' influence on GFSAs' samples produced by Littelfuse and EPCOS like investigation done for xenon-filled tube published in [27] as well as given the current attractiveness of investigations based on radiation of different types of components [28-30].

Acknowledgement: *This work has been supported by the Ministry of Education, Science and Technological Development of the Republic of Serbia.*

REFERENCES

[1] M. M. Pejović, *Introduction to electrical gas discharges. Gas electronic components*, in Serbian, University of Niš, Faculty of Electronic Engineering, 2008, Chapter 8, pp. 124-128.
[2] https://www.littelfuse.com/~/media/electronics/product_catalogs/littelfuse_gdt_catalog.pdf.pdf
[3] https://www.tdk-electronics.tdk.com/inf/100/ds/A81-A230XG-X3800T502.pdf
[4] E. Živanović, S. Veljković, M. Živković amd M. Pejović, "Reliability of various type of gas-filled surge arresters under DC discharge", In Proceedings of the 31st International Conference on Microelectronics, Niš, Serbia, 2019, pp. 113-116.
[5] K. Stanković and L. Perazić, "Determination of gas-filled surge arresters lifetimes", *IEEE Trans. on Plasma Sci.*, vol. 47, no. 1, pp. 935-943, January 2019.
[6] J. He, J. Lin, W. Liu, H. Wang, Y. Liao and S. Li, "Structure-dominated failure of surge arresters by successive impulses", *IEEE Trans. on Power Delivery*, vol. 32, no. 4, pp. 1907-1914, August 2017.
[7] B. Lončar, P. Osmokrović, A. Vasić and S. Stanković "Influence of gamma and X radiation on gas-filled surge arrster characteristics", *IEEE Trans. Plasma Sci.*, vol. 34, no. 4, pp. 1561-1565, August 2006.
[8] B. Lončar, M. Vujisić, K. Stanković, D. Arandić and P. Osmokrović, "Radioactive resistance of some commercial gas filled surge arresters", In Proceedings of the 26th International Conference on Microelectronics, Niš, Serbia, 2008, pp. 587–590.
[9] M. M. Pejović and M. M. Pejović, "Investigations of breakdown voltage and time delay of gas-filled surge arresters", *J. Phys. D: Appl. Phys.*, vol. 39, pp. 4417-4422, September 2006.
[10] M. M. Pejović, K. Stanković, I. Fetahović, M. M. Pejović, "Processes in insulating gas induced by electrical breakdown responsible for commercial gas-filled surge arresters delay response", *Vacuum*, vol. 137, pp. 85-91, March 2017.
[11] Y. Fu, P. Zhang, J. P. Verboncoeur and X. Wang, "Electrical breakdown from macro to micro/nano scales: a tutorial and a review of the state of the art", *Plasma Res. Express*, vol. 2, p. 013001, February 2020.

[12] Z. Lj. Petrović, J. Sivoš, M. Savić, N. Škoro, M. Radmilović Rađenović, G. Malović, S. Gocić and D. Marić, "New phenomenology of gas breakdown in DC and RF fields", *J. Phys.: Conf. Series*, vol. 514, p. 012043, May 2014.

[13] S. Gocić, N. Škoro, D. Marić and Z. Lj. Petrović, "Influence of the cathode surface conditions on V–A characteristics in low-pressure nitrogen discharge", *Plasma Sources Sci. Technol.*, vol. 23, p. 035003, May 2014.

[14] D. Marić, N. Škoro, P. D. Maguire, C. M. O. Mahony, G. Malović and Z. Lj. Petrović, "On the possibility of long path breakdown affecting the Paschen curves for microdischarges", *Plasma Sources Sci. Technol.*, vol. 21, p. 035016, May 2012.

[15] A. M. Loveless and A. L. Garner, "A universal theory for gas breakdown from microscale to the classical Paschen law", *Physics of Plasmas*, vol. 24, p. 113522, November 2017.

[16] M. M. Pejović, Č. S. Milosavljević and M. M. Pejović, "The estimation of static breakdown voltage for gas-filled tubes at low pressures using dynamic method", *IEEE Trans. Plasma Sci.*, vol. 31, pp. 776-781, August 2003.

[17] J. M. Meek and J. D. Craggs, *Electrical breakdown of gases*, New York, USA: Wiley, 1987.

[18] M. M. Pejović, G. S. Ristić and J. P. Karamarković, "Electrical breakdown in low pressure gases", *J. Phys. D: Appl. Phys*., vol. 35, pp. R91-R103, April 2002.

[19] M. M. Pejović, M. M. Pejović, Č. I. Belić, K. Đ. Stanković, "Separation of vacuum and gas breakdown processes in argon and their influence on electrical breakdown time delay", *Vacuum*, vol. 173, p. 109151, March 2020.

[20] M. M. Pejović, "The application of a small-volume neon-filled tube in overvoltage protection", *IEEE Trans. on Plasma Sci*., vol. 43, no. 4, pp. 1063-1067, April 2015.

[21] M. Pejović, K. Stanković, M. Pejović and P. Osmokrović, *Processes induced by electrical breakdown responsible for the memory effect in low pressure noble gases*, in book Advances in chemistry research, 2019, Chapter 2, vol. 47, edited by J. C. Taylor, New York: Nova science Publishers, Inc., pp. 47-93.

[22] E. N. Živanović, "Investigation of the effect of additional electrons originating from the ultraviolet radiation on the nitrogen memory effect", *FU Elec. Energ.*, vol. 28, no. 3, pp. 423-437, September 2015.

[23] M. M. Pejović, N. T. Nesić, M. M. Pejović and E. N. Živanović, "Afterglow processes responsible for memory effect in nitrogen", *J. Appl. Phys.*, vol. 112, p. 013301, May 2012.

[24] E. N. Živanović, "Influence of combined gas and vacuum breakdown mechanisms on memory effect in nitrogen", *Vacuum*, vol. 107, pp. 62-67, September 2014.

[25] E. N. Živanović, M. M. Pejović, M. M. Pejović and N. T. Nešić, "Analysis of the statistical nature of electrical breakdown time delay in nitrogen at 6.6 mbar pressure in presence of positive ions and N(^{4}S) atoms", *Contrib. to Plasma Phys.*, vol. 51, no. 9, pp. 877-884, April 2011.

[26] F. Llewellyn Jones, E. T. de la Perrelle, "Field Emission of Electrons in Discharges", *Proc. Math. Phys. Eng. Sci.*, vol. 216, no. 1125, pp. 267-279, January1953.

[27] M. Pejović, E. Živanović and M. Živanović, "Investigation of xenon-filled tube breakdown voltage and delay response as possible dosimetric parameters for small gamma ray air kerma rates", *Radiat. Prot. Dosim.*, vol. 190, no. 1, pp. 84-89, August 2020.

[28] D. Boychenko, O. Kalashnikov, A. Nikiforov, A. Ulanova, D. Bobrovsky and P. Nekrasov, "Total ionizing dose effects and radiation testing of complex multifunctional VLSI devices", *FU Elec. Energ.*, vol. 28, no. 1, pp. 153-164, March 2015.

[29] M. Pejović, "P-channel MOSFET as a sensor and dosimeter of ionizing radiation", *FU Elec. Energ.*, vol. 29, no. 4, pp. 509-541, December 2016.

[30] T. Pešić-Brđanin, "Spice modeling of ionizing radiation effects in CMOS devices", *FU Elec. Energ.*, vol. 30, no. 2, pp. 161-178, June 2017.